Adaptive Ping Control for Track-Holding in Multistatic Active Sonar Networks

Cherry Y. Wakayama
Code 56560
SPAWAR Systems Center Pacific
San Diego, CA, U.S.A.
cherry.wakayama@navy.mil

Doug J. Grimmett
Code 56560
SPAWAR Systems Center Pacific
San Diego, CA, U.S.A.
grimmett@spawar.navy.mil

Abstract – *Distributed multistatic active sonar networks provide an Anti-Submarine Warfare capability against small, quiet, threat submarines in the harsh clutter-saturated littoral and deeper ocean environments. Adaptive ping control techniques provide the potential to significantly increase the multistatic network's performance, by pinging (in an optimum sense) the right source, at the right time, with the right waveform. This paper describes an automatic, adaptive ping control algorithm. It specifically addresses the "track-hold" objective, which is to adapt multistatic sonar operations to maintain and hold one or more target tracks which have been previously initiated (detected). The approach is unique in that it includes both sonar performance modeling and multistatic tracker outputs, in a closed-loop control structure. The paper motivates the approach, describes the algorithm, and shows some validating results. The evaluation utilizes a simple sonar performance model, a ping contact simulator, and a multistatic target tracker. Results are shown for a simple simulated scenario, showing the advantages of this adaptive ping control algorithm compared to using a pre-planned, non-adaptive ping transmission schedule.*

Keywords: Sensor management, ping management, ping control, sonar optimization, multistatic tracking, sonar performance modeling.

1 Introduction

Distributed multistatic active sonar networks have the potential to increase Anti-Submarine Warfare (ASW) performance against small, quiet, threat submarines in the harsh clutter-saturated littoral and deeper ocean environments. This improved performance comes through the expanded geometric diversity of a distributed field of sources and receivers and results in increased probability of detection, area coverage, target tracking, classification, and localization [1]. However, given the variability in environmental (acoustic) conditions, sonar node performance (as a function of location, time, and other parameters), and threat target

behavior, such networks will not exploit their full potential without intelligent management and control methods. Adaptive sonar control techniques and tactical decision aides may be applied to best address the following questions: Where?, Which?, What?, When?, and How? The **Where** question is addressed through multistatic sensor placement algorithms. The **How** question is addressed by adaptive signal and information processing algorithms. The **Which**, **What**, and **When** are applicable to sonar ping control algorithms as explained below.

- **Which** source(s) to transmit – The attempt is to optimally choose which source or sources of all those in the field are best to ping next, given the objectives and current status of the ASW mission being executed. Current methods typically employ a regular, cyclic, pre-planned ping transmission schedule, which is often arbitrarily determined and not specifically optimized for achieving the ASW objective. An adaptive solution will attempt to increase ASW coverage, as well as consider other factors such as field persistence and energy constraints [2, 3].

- **What** waveform(s) to transmit – Given environmental conditions, sonar geometry, and target behavior, an optimum selection of transmission waveform may be made. Center frequency, bandwidth, and pulse duration are important signal characteristics which may be controlled and optimized for the multistatic field; sonar performance modeling will enable an optimization algorithm to make the best selection. An important element of this is the choice between Doppler-sensitive (eg. CW) and Doppler-insensitive (eg. FM) waveforms. It has been shown that these waveform types provide complementary performance within a multistatic field [4], and therefore their selection should be made in an intelligent, optimized way.

- **When** to transmit the source – This may address the operational persistence of the field, by intelli-

Report Documentation Page	*Form Approved* *OMB No. 0704-0188*

Public reporting burden for the collection of information is estimated to average 1 hour per response, including the time for reviewing instructions, searching existing data sources, gathering and maintaining the data needed, and completing and reviewing the collection of information. Send comments regarding this burden estimate or any other aspect of this collection of information, including suggestions for reducing this burden, to Washington Headquarters Services, Directorate for Information Operations and Reports, 1215 Jefferson Davis Highway, Suite 1204, Arlington VA 22202-4302. Respondents should be aware that notwithstanding any other provision of law, no person shall be subject to a penalty for failing to comply with a collection of information if it does not display a currently valid OMB control number.

1. REPORT DATE **JUL 2010**	2. REPORT TYPE	3. DATES COVERED **00-00-2010 to 00-00-2010**

4. TITLE AND SUBTITLE	5a. CONTRACT NUMBER
Adaptive Ping Control for Track-Holding in Multistatic Active Sonar Networks	5b. GRANT NUMBER
	5c. PROGRAM ELEMENT NUMBER
6. AUTHOR(S)	5d. PROJECT NUMBER
	5e. TASK NUMBER
	5f. WORK UNIT NUMBER
7. PERFORMING ORGANIZATION NAME(S) AND ADDRESS(ES) **SPAWAR Systems Center Pacific,Code 56560,San Diego,CA**	8. PERFORMING ORGANIZATION REPORT NUMBER
9. SPONSORING/MONITORING AGENCY NAME(S) AND ADDRESS(ES)	10. SPONSOR/MONITOR'S ACRONYM(S)
	11. SPONSOR/MONITOR'S REPORT NUMBER(S)

12. DISTRIBUTION/AVAILABILITY STATEMENT
Approved for public release; distribution unlimited

13. SUPPLEMENTARY NOTES
Presented at the 13th International Conference on Information Fusion held in Edinburgh, UK on 26-29 July 2010. Sponsored in part by Office of Naval Research, Office of Naval Research Global, and U.S. Army Research Laboratory's Army Research Office (ARO). U.S. Government or Federal Rights License.

14. ABSTRACT
Distributed multistatic active sonar net- works provide an Anti-Submarine Warfare capability against small, quiet, threat submarines in the harsh clutter-saturated littoral and deeper ocean environ- ments. Adaptive ping control techniques provide the potential to signi cantly increase the multistatic net- work's performance, by pinging (in an optimum sense) the right source, at the right time, with the right wave- form. This paper describes an automatic, adaptive ping control algorithm. It speci cally addresses the rack- hold" objective, which is to adapt multistatic sonar op- erations to maintain and hold one or more target tracks which have been previously initiated (detected). The ap- proach is unique in that it includes both sonar perfor- mance modeling and multistatic tracker outputs, in a closed-loop control structure. The paper motivates the approach, describes the algorithm, and shows some val- idating results. The evaluation utilizes a simple sonar performance model, a ping contact simulator, and a multistatic target tracker. Results are shown for a sim- ple simulated scenario, showing the advantages of this adaptive ping control algorithm compared to using a pre- planned, non-adaptive ping transmission schedule.

15. SUBJECT TERMS

16. SECURITY CLASSIFICATION OF:			17. LIMITATION OF ABSTRACT	18. NUMBER OF PAGES	19a. NAME OF RESPONSIBLE PERSON
a. REPORT **unclassified**	b. ABSTRACT **unclassified**	c. THIS PAGE **unclassified**	**Same as Report (SAR)**	**8**	

Standard Form 298 (Rev. 8-98)
Prescribed by ANSI Std Z39-18

gently selecting ping times to preserve sources' energy stores [3]. It may also provide fine-tuned ping timing commands, which attempt to capture targets while in (relatively rare) specular target geometries. Targets ensonified while in the specular (beam aspect) geometry produce very loud (more than one order of magnitude greater) detection echoes [5]. Specular echoes have demonstrated extreme value in multistatic data fusion, tracking, and classification algorithms [6]. Adaptive ping control may attempt to capture such opportunities through precise ping timing without which they would otherwise be missed.

In considering adaptive ping control, it is important to understand the possible ASW objectives, or mission modes of operation under which it may be applied. Typical operations can be grouped into the following mission modes:

- **Target Search Mode** – In this mode, the surveillance operation is focused on optimizing performance in detecting targets and initiating tracks on these detections. The objective is to detect the (unknown number of) targets in a surveillance area. This applies to monitoring a surveillance barrier for penetration, or wide area search and clearing (sanitization) missions. Intelligent ping management for target search has been addressed in the literature [2, 3].

- **Track-Holding Mode** – In this mode, the operation is focused on holding tracks and maintaining good localization estimates for targets which have already been detected. Here, it is assumed that highly probably detection threat(s) have been detected, with confirmed tracks initiated, and the objective is to do everything possible not to lose these targets. This objective is important to enable target contact confirmation and classification, and to provide localization cueing solutions to other sensors or sensor networks. It can also contribute to targeting solutions for effective prosecution.

- **Search and Hold Mode** – This mode attempts to perform the previous two modes in parallel. An optimization solution would need to consider both objectives, which may or may not be competing, within the solution space.

This paper describes an automatic, adaptive ping control optimization algorithm, which is designed specifically to address the "track-hold" operation. It provides a comprehensive control solution to all three of the ping management questions in parallel: which source to ping, what waveform type (Doppler-sensitive continuous wave (CW) or Doppler-insensitive frequency-modulated wave (FM)) to use, and when to ping in order to capture high-strength specular detection echoes. The approach is unique in that it considers both sonar performance prediction modeling, and

fused multistatic tracker outputs in a closed-loop control structure. The ping control commands are generated by the control generator which takes inputs from a simple sonar performance model [4, 7] as well as the output tracks of a multistatic tracker [6, 8, 9]. This paper proceeds as follows: Section 2 describes the adaptive ping control architecture, Section 3 describes the ping control generator, Section 4 shows some validating results on a simple simulated scenario, and Section 5 provides conclusions and recommendations.
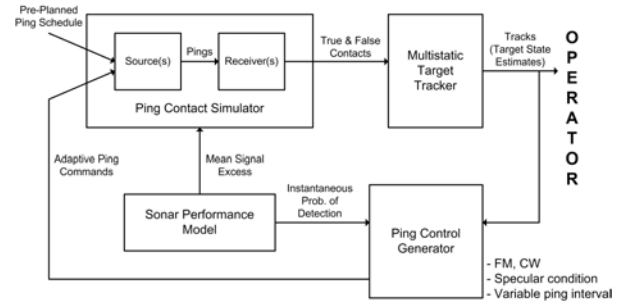
2   Adaptive Ping Control Architecture

Figure 1: Adaptive ping control architecture.

The adaptive ping control architecture is based on principles of Feedback Control of dynamical systems with uncertainty parameters. In this architecture, the target information is obtained by sensor measurements and processed by the tracker and the control generator, and the processed information is then fed back to the sensor network for improved tracking. A diagram of the adaptive ping control architecture is shown in Figure 1. This architecture consists of four main modules: Sonar Performance Model, Ping Contact Simulator, Multistatic Target Tracker, and Ping Control Generator. The sonar performance model (SPM) computes mean signal-to-noise ratios (SNR) or signal excesses (SE) for given field configurations, consisting of sources, receivers and moving targets. The ping contact simulator generates contacts which represent true (target-originated) and false echo detections at each receiver for each processed sonar ping. The multistatic target tracker computes current and future state estimates based on sensor data and target and measurement uncertainty and produces tracks. The ping control generator generates ping commands as a function of the tracker's current state estimate and predictions (future state estimates), control parameters, and sonar performance model predictions. We briefly describe the sonar performance model, the ping contact simulator, and the tracker in the follow-

ing subsections and the control generator is discussed in detail in Section 3.

2.1 Sonar Performance Model

The sonar performance model provides mean levels of SNR, which are used by the ping control generator, and is an essential element of the ping control simulation module. Accurate modeling of sonar system performance is non-trivial, given the complexity and uncertain knowledge of the underwater acoustic environment. Here, we choose to use a simple bistatic sonar performance model [4], which is sufficient in capturing the gross features important to this analysis. Future studies may incorporate higher fidelity acoustic sub-models into the approach, as needed. A wholly reverberation-limited shallow water environment is assumed, being dominated by sea bottom reflections. Transmission losses to/from the target and the bottom underneath it are assumed equivalent. CW and FM waveforms are modeled using their respective Q-functions (descriptions of their performance against reverberation) [4]. Aspect-dependent Target Strength is modeled, and includes high-strength echoes when the target is in the specular condition [7]. The specular geometric condition occurs when the angles from the target to the source and receiver are equal (fore and aft, or, aft and fore) from the target's beam angle ($\pm 90°$ from the target's heading). Levels of mean SNR for a single ping received by the entire field are output, given bistatic source-receiver geometries, assumed target speeds and headings, and other parameters.

2.2 Ping Contact Simulator

A simulator is required in order to test and evaluate the ping control algorithm. This module provides contact (scan) files for each receiver, given a waveform transmission from a particular acoustic source. The modeled contacts consist of both target-originated contacts and false alarm contacts, and the resulting scan files may be input into the multistatic tracker. The simulator may be driven by the adaptive ping control algorithm, or by a pre-planned ping schedule (which may be done to provide a comparison baseline). Each contact contains the following information: source and receiver identification, waveform type, ping time, SNR, bearing, arrival time (for ranging), and range-rate (if CW). Target contacts are derived from a manufactured scenario of target truth trajectories. They are modeled by obtaining mean SNR from the sonar performance model, and adding a random fluctuation term (σ_{SE}) from a Gaussian distribution (nominally 0 mean and 5 dB fluctuation), along with assumed measurement (bearing, time, and range-rate) errors. A number of false target contacts (nominally 50) are generated for each sonar scan, with a uniform distribution in time-bearing measurement space, and a Gaussian distribution for bistatic range-rate. For this study, false contact SNRs were modeled assuming a Gaussian distribution (nominally 12 dB mean and 5 dB fluctuation).

2.3 Multistatic Target Tracker

The multistatic tracker generates target state estimates from measurements and associates target contacts to form tracks. In this work, we use a centralized, Kalman Filter tracker [6, 8]. The input to the tracker is a series of contact files (measurement scans), unique to each source-receiver-waveform and time of ping transmission provided by the ping contact simulator. Target motion is modeled using a 2-dimensional *nearly constant velocity* motion model. Converted, de-biased positional measurements are used together with range-rate measurements in an extended Kalman Filter (EKF). A logic-based track initiation (M/N) and termination (K) scheme is used. Nearest neighbor data association is used, with a 2-dimensional or 3-dimensional (if Doppler measurements are available) ellipsoidal association gate. Target state updates for the track-set selected for holding are provided to the ping control generator. The improvements in target holding seen at the output of the tracker is a measure of the success of the ping control algorithm.

3 Ping Control Generator

The ping control generator uses current and future state estimates from the tracker, the sonar performance model, and control objectives to derive an optimal ping command which consists of source, waveform, and ping-time selection. In this formulation, we consider only the track-holding scenario, where confirmed tracks have already been established by the tracker. The objective of the control generator is to maximize the instantaneous detection probability of the target tracks at the input and output of the tracker for effective holding of the targets. The strategy is to focus on regions of the state space with higher likelihood of future target presence and maximize the target detection probability by intelligent ping management. This approach is illustrated in Figure 2.

3.1 Variable Ping Interval

The current ping time is denoted by t_k. We define the minimum and maximum ping intervals, $\Delta t_{\min}$ and $\Delta t_{\max}$. We consider a forecast window of width T with time increment ΔT and the forecast time $t_p \in \{t_k + \Delta t_{\min}, t_k + \Delta t_{\min} + \Delta T, \cdots, t_k + \Delta t_{\min} + T\}$. The next ping time, t_{k+1}, is selected from the set $\{t_k + \Delta t_{\min}, t_k + \Delta t_{\min} + \Delta T, \cdots, t_k + \Delta t_{\max}\}$. The descriptions of the time variables mentioned above are given in Figure 3. Here, we consider up to the time $\Delta t_{\max} + \Delta t_{\min}$ from the current ping time, t_k, because there is a minimum lock-out period $\Delta t_{\min}$ required before generating the next ping to wait for sonar ping returns and to conserve available energy of the sources.
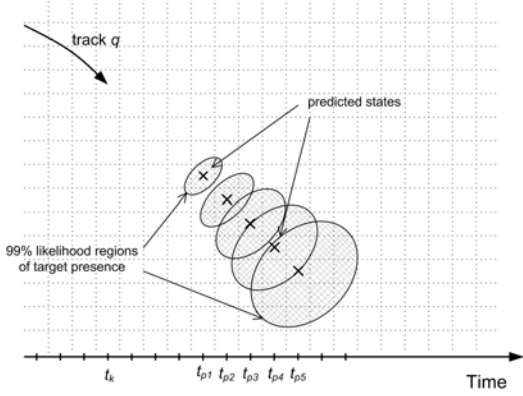
Figure 2: A depiction of the approach.

If the best ping interval, t_p^*, is predicted to fall between $t_k + \Delta t_{\min}$ and $t_k + \Delta t_{\max}$, the next ping time is set to t_p^*. If t_p^* falls between $t_k + \Delta t_{\max}$ and $t_k + \Delta t_{\max} + \Delta t_{\min}$, we select the best next ping time, t_{k+1}, from the set $\{t_k + \Delta t_{\min}, t_k + \Delta t_{\min} + \Delta T, \cdots, t_k + t_p^* - \Delta t_{\min}\}$. The variable ping interval mechanism allows the fine tuning of the ping time in order to capture the specular geometric condition which occurs fleetingly. Although the specular geometry is rare, when this configuration occurs, it yields a very high strength target echo relative to other geometries, and therefore should be exploited when a specular opportunity is expected [5].
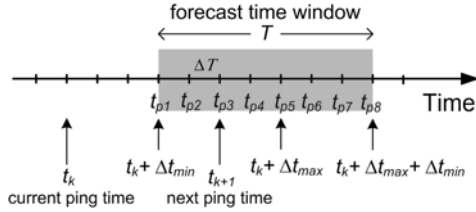

Figure 3: Variable Ping Interval.

3.2   Track Forecast

For each forecast time, t_p, the optimal estimate (under linear Gaussian assumptions of Kalman filtering) of the target state and its covariance matrix are predicted by the multistatic target tracker as [8]:

$$X(p|k) = \Phi(t_p - t_k)X(k|k), \tag{1}$$

$$P(p|k) = \Phi(t_p - t_k)P(k|k)\Phi^T(t_p - t_k) + Q(t_p - t_k), \tag{2}$$

where $X(k|k) = [\hat{x}(t_k), \hat{y}(t_k), \hat{\dot{x}}(t_k), \hat{\dot{y}}(t_k)]^T$ is the state estimate (position and velocity in the Cartesian coordinate system) at time t_k and $P(k|k)$ is its error covariance matrix, $\Phi(t_p - t_k)$ is the discrete-time state

transition matrix from time t_k to t_p, and $Q(t_p - t_k)$ is the covariance matrix associated with the zero-mean white Gaussian noise process for a *nearly constant velocity* target motion model. $X(p|k)$ is the linear optimal prediction at t_p and $P(p|k)$ is the error covariance matrix associated with $X(p|k)$.

3.3   Discretization of Likelihood Region

At each forecast time, the likelihood region of target state is described by the hyper-ellipsoid which is defined by the eigenvalues of the covariance matrix $P(p|k)$. In order to characterize the target state within the hyper-ellipsoid, we discretize the ellipsoid into a 4-dimensional grid $\{X_i = (x_i, y_i, \dot{x}_i, \dot{y}_i), i = 1, \cdots, N_L^p\}$, where N_L^p is the total number of grid cells in the likelihood region at time t_p. We use a 3σ likelihood region at each forecast time which corresponds to a target state probability $(1 - \alpha)$ of 99%. The contour delineating the region of constant probability α about $X(p|k)$ is given by the value of a chi-square random variable z with 4 degrees of freedom which satisfies

$$P\left(z \leq \chi_4^2(\alpha)\right) = 1 - \alpha. \tag{3}$$

3.4   Optimization Criteria

To perform optimum track-holding, we choose a ping command, u (source, waveform, ping time), that maximizes the instantaneous probability of target detection at the tracker input weighted by the probability of target presence and the tracker association probability due to false alarms. The optimization criteria for each target state grid cell of each active track at each forecast time is given by

$$P_{TR}(X_i, X_j^R, u) = P_T(X_i) \times P_D(X_i, X_j^R, u) \times P_A(u), \tag{4}$$

where $P_{TR}(X_i, X_j^R, u)$ is the grid cell probability that the tracker will associate the target-originated detection by receiver j if action u is taken and the target state is X_i; $X_j^R = (x_j^R, y_j^R, \dot{x}_j^R, \dot{y}_j^R)$ denotes the state of receiver j. $P_T(X_i)$ is the probability that the target state is X_i. $P_D(X_i, X_j^R, u)$ is the probability of detection at the tracker input corresponding to X_j^R, if the target state is X_i and action u is taken. $P_A(u)$ is the probability of tracker association of a target-originated detection if action u is taken for a given false alarm rate. Each probability in Eq. (4) is defined as follows:

- **Probability of target state** – The density function for the target state X_i at t_p is given by the quadravariate normal distribution with mean vector $\mu = X(p|k)$ and covariance matrix $\Sigma = P(p|k)$ computed by the tracker as

$$f(X_i) = \frac{1}{(2\pi)^2 \sqrt{|\Sigma|}} \exp\left[-\frac{1}{2}(X_i - \mu)^T \Sigma^{-1}(X_i - \mu)\right]. \tag{5}$$

The probability of the target state being within each grid cell $P_T(X_i)$ is obtained by integrating the density function over the grid cell.

- **Tracker detection probability** – For each target state X_i, the corresponding mean SNR for each source-receiver-waveform triple is computed using the simple sonar performance model as described in Section 2.1. The mean signal excess, $\overline{SE}$ (in dB), is computed as the difference between the mean SNR and the tracker classifier threshold (TH). We model the signal excess fluctuations by a normal distribution function, with standard deviation σ_{SE} of about its mean $\overline{SE}$. The relationship between signal excess and detection probability for the normal fluctuation model is given in [10]. The detection probability is approximated by a simpler expression as

$$P_D(X_i, X_j^R, u) = \frac{1}{2}\left(1 + \text{erf}\left(\frac{\overline{SE}\left(X_i, X_j^R, u\right)}{\sqrt{2}\sigma_{SE}}\right)\right). \tag{6}$$

- **Tracker association probability** – After each ping time, multiple contacts are generated at each receiver, the collection of which are called a scan, due to a given false alarm rate. For each scan, a validation gate centered around the predicted measurement of the track is set up to select the correct measurement from the target probabilistically. We compute the area of validation gate at each forecast time, since the validation gate gets larger and the number of false alarms in the validation ellipsoid increases as the forecast interval increases. In order to account for increased uncertainty at later forecast times, we include the track association probability in the optimization criteria (4). We make the following assumptions to simplify the computation of P_A: (1) the false alarm rate is constant at each scan, (2) false alarms are distributed uniformly in the area $\mathcal{A}^\tau$ defined by the bistatic ellipse formed by the source and receiver pair in consideration and the listening-time parameter, (3) any measurement within the validation gate can be associated by the tracker with equal probability, and (4) there is one target-originated detection in the validation gate (due to a 99% validation gate).

The error ellipsoid associated with each forecast is given by the covariance matrix $S(p) = C(p)P(p|k)C^T(p) + R(p)$, where C and R are the corresponding Jacobian measurement matrix and the measurement error matrix, respectively [6, 8]. For an FM source, $S \in \mathbb{R}^{2\times 2}$ and for a CW source, $S \in \mathbb{R}^{3\times 3}$. Let A denote the cross-sectional area of the error ellipsoid defined by S. The total number of false alarms per scan is denoted by N_{fa}. We use superscripts fm or cw to denote an FM or CW waveform, respectively. The tracker association probabil-

ity for an FM source is approximated by

$$P_A^{fm} = \frac{1}{1 + N_{fa}^{fm} \cdot A^{fm}/\mathcal{A}^\tau}. \tag{7}$$

For a CW source, we model the bistatic range rate of false alarms, denoted by $\tilde{r}$, by a normal distribution with density $\tilde{f}(\tilde{r})$ and assume false alarm range rate is independent of positional measurements. We approximate $\sigma_{x\tilde{r}}$ and $\sigma_{y\tilde{r}}$ of S^{cw} to be zero. The tracker association probability for a CW source is approximated by

$$P_A^{cw} = \frac{1}{1 + F \cdot N_{fa}^{cw} \cdot A^{cw}/\mathcal{A}^\tau}, \tag{8}$$

$$F = \int_{\bar{\tilde{r}}-c}^{\bar{\tilde{r}}+c} \tilde{f}(\tilde{r})\mathrm{d}\tilde{r}, \tag{9}$$

where $\bar{\tilde{r}}$ is the expected value of target range rate and c is the length of semi-axis of the error ellipsoid corresponding to the bistatic range rate.

3.5 Objective Function

The objective of the control generator is to choose the next ping command (source, waveform, ping time) which maximizes the tracker's detection performance metric. The metric includes the case of multiple active tracks. For each active track forecast and each receiver, we compute the total sum of grid cell (tracker detection) probability within the error ellipsoid defined by $P(p|k)$. The maximum is selected amongst all receivers, weighted, and then summed over all the active tracks. The potential ping command with the maximum performance metric is chosen. The performance metric is given by

$$g_m = \sum_{q}^{N_{TR}} \beta_q(k) \max\left(h_1, h_2, \cdots, h_{N_R}\right), \tag{10}$$

$$h_j = \sum_{i}^{(N_L^p)^q} P_{TR}^q\left(X_i, X_j^R, u_m\right), \tag{11}$$

$$u_m \in \{(\text{source, waveform, ping time})\}, \tag{12}$$

where N_{TR} is the number of active tracks to hold at the current time t_k, N_R is the number of receivers, and $\beta_q(k)$ is the weighting parameter for each active track q at t_k, and $(N_L^p)^q$ is the total number of grid cells in the likelihood region associated with track q at time t_p. The weighting parameter $\beta_q(k)$ is computed as

$$\beta_q(k) = L_q(k)\left(1 - \frac{\bar{d}_q^2(k)}{\sum_i^{N_{TR}} \bar{d}_i^2(k)}\right), \tag{13}$$

where $L_q(k)$ is the length of the active track q at time t_k and $\bar{d}_q^2(k)$ represents the normalized, averaged norm of the residual of the track q weighted by the corresponding covariance matrix $S^q(i), i = 1, \cdots, k$ at each ping time, t_i.

In Eq. (10), we choose the maximum total detection probability resulting from all receivers in order to emphasize the specular geometric opportunity. One could also choose the average value over all or a set of receivers if cross-fixing is considered in the tracker.

4   Simulation

The use of different waveforms within a geographically distributed multistatic network offers diversity in target tracking opportunities [4]. Targets traveling with a heading along (or tangential to) the bistatic equi-time ellipses present a specular condition with a large enhancement of target strength, but a zero-Doppler shift to the source-receiver pair. On the other hand, targets traveling with a heading orthogonal to the ellipses present the maximum target Doppler shift to the source-receiver pair, but a relatively low target strength. In this section, we demonstrate the exploitation of waveform and geometric diversity for tracking by adaptive ping control which includes source, waveform, and ping time selection. We present two simulation examples: the first example is simulated without any false alarms and without target SNR fluctuations, and the second example with false alarms and with target SNR fluctuations.
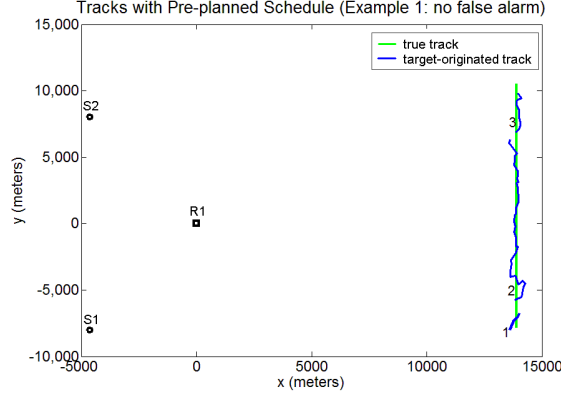

Figure 4: Tracking result with the pre-planned schedule for no false alarm case.

4.1   Example 1: No false alarm

In this example, there are 2 sources and 1 receiver deployed in the field and their positions are stationary. A target of interest is heading north with a constant speed of 5 knots. The scenario is illustrated in Figure 4. The input parameters for the tracker are as follows: $M = 3$, $N = 4$ for track confirmation, $K = 2$ for track termination, association gate value $(1-\alpha) = 99\%$, tracker classifier threshold $TH = 10$ dB, maneuverability index of 0.01 m^2/s^3, error of receiver bearing of 2°, error of receiver timing of 0.02 seconds, error of
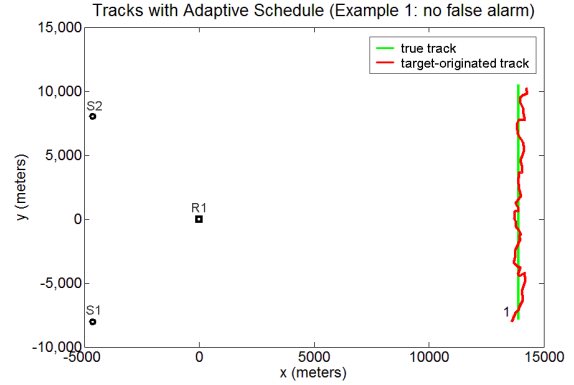

Figure 5: Tracking result with the adaptive schedule for no false alarm case.

bistatic range rate of 0.1 m/s, and error of speed of sound of 15 m/s. Figures 4 and 5 show the tracking results with a pre-planned schedule and an adaptive ping schedule, respectively. The pre-planned schedule is given by a simple round-robin scheme in which each ping is generated from the source and waveform combination of {(S1,FM),(S2,FM),(S1,CW),(S2,CW)} with a constant ping interval of 60 seconds. With the pre-planned schedule in Figure 4, we can see that it results in fragmented target tracks. We initiate the adaptive schedule scheme with the pre-planned schedule until there is a confirmed track. The minimum and maximum ping intervals for the adaptive scheme are set to 60 seconds and 90 seconds, respectively, with a 15 second increment. The adaptive schedule scheme not only continuously holds the target without fragmentation, but provides higher detection SNRs to the tracker.
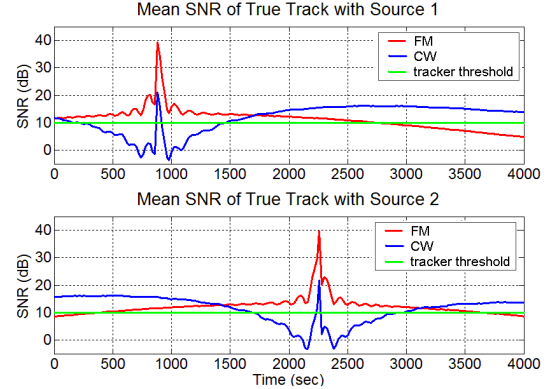

Figure 6: Mean SNR levels of true target generated by each source and waveform combination.

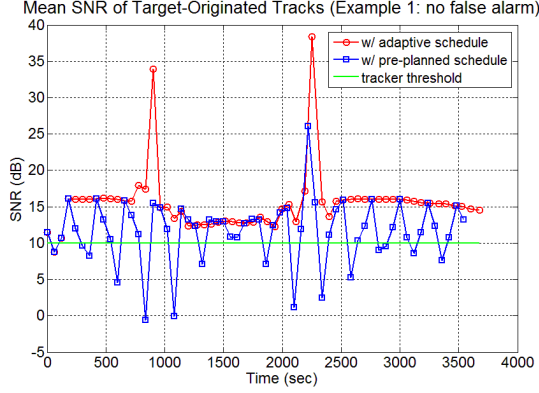Figure 6 shows the mean SNR levels (prior to the

Figure 7: Comparison of the tracker input mean SNR (without fluctuations) resulting from the pre-planned schedule and the adaptive schedule.
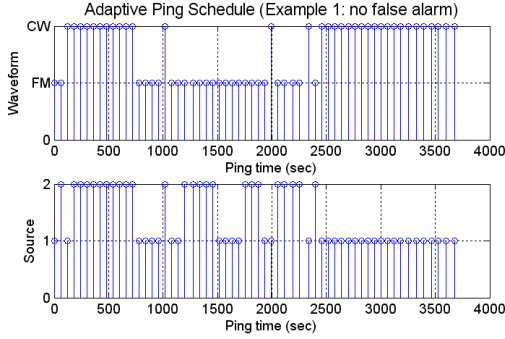

Figure 8: Adaptive ping schedule for no false alarm case.

addition of SE fluctuations) of the true target track for each source and waveform combination. We see two specular opportunities, first with Source 1 ($\sim$ 900 sec) and later with Source 2 ($\sim$ 2250 sec). Away from the specular, the CW provides better echo strength. We expect the adaptive ping algorithm to automatically exploit these trends. Figure 7 shows the comparison between target-originated mean SNR using the pre-planned schedule and the adaptive schedule. We see that the adaptive schedule captures both specular events where the pre-planned schedule only partially captures one. In addition, the average increase in mean SNR is about 4 dB for this case. The resulting adaptive schedule is shown in Figure 8. As expected, the FM waveforms is more often selected during the middle of the run, including the period when the specular detections occur. At the beginning and end of the run the CW is more prominent. Also, Source 2 is selected more often at the beginning and Source 1 at the end, in accordance with the target's Doppler presented to the respective sources as it moves along its track.

4.2   Example 2: With False Alarms

In this example, we simulate the same scenario with the same parameters as described in the previous example, except we generate 50 false alarms per scan for both FM and CW pings and add target SNR flucations ($\sigma_{SE} = 5$ dB). The false alarm generation is briefly described in Section 2.2.
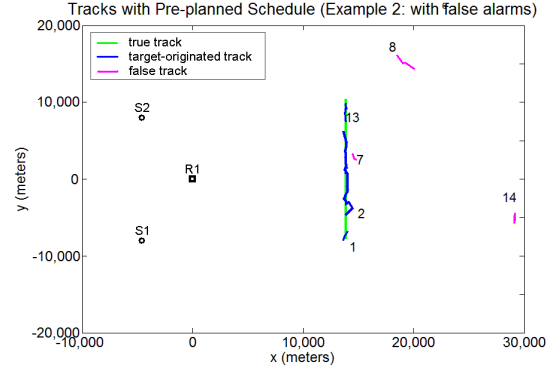

Figure 9: Tracking result with the pre-planned schedule for 50 false alarms per scan case. Note that only 3 out of 11 false tracks are present in the region displayed.
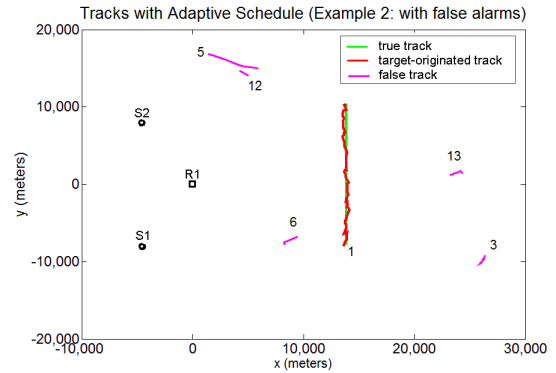

Figure 10: Tracking result with the adaptive schedule for 50 false alarms per scan case. Note that only 5 out of 12 false tracks are present in the region displayed.

The simulation results are shown in Figures 9 - 12. We observe that with false alarms, some false tracks are confirmed. However, they are eventually rejected. Here again, the pre-planned schedule results in fragmented target tracks. Even with false tracks, the adaptive schedule scheme results in the continuous holding of the target track, although the second specular opportunity is missed. This may be due to the effect of multiple active tracks, SE fluctuations, and/or ping

time interval and grid size resolutions. Nevertheless, the benefit and potential of the adaptive ping control algorithm is clearly seen. For more realistic and challenging scenarios, we expect the algorithm to provide additional improvement in track-hold time, along with the tracker's fragmentation reduction shown here.
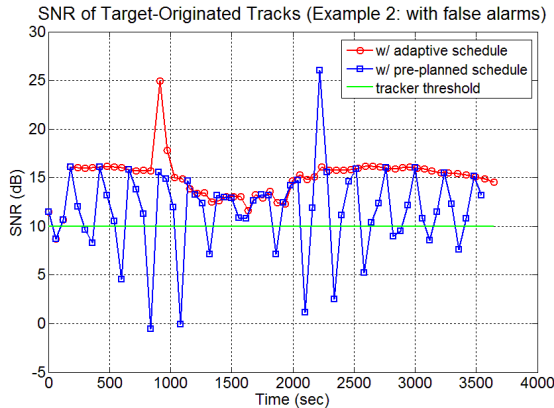

Figure 11: Comparison of the tracker input SNR (with 5 dB fluctuations) with the pre-planned schedule and the adaptive schedule for 50 false alarms per scan case.
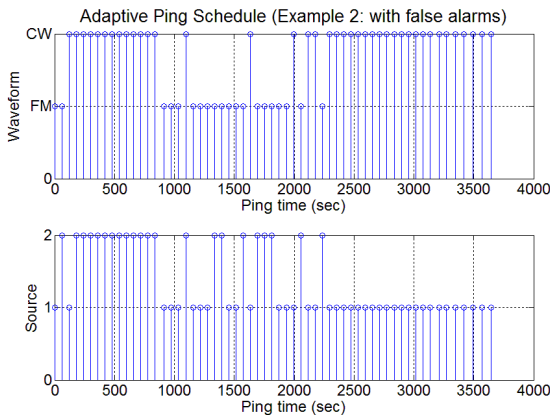

Figure 12: Adaptive ping schedule for 50 false alarms per scan.

5   Conclusions and Future Work

We have presented an adaptive ping control framework for the track-holding scenario. Our main objective is to improve the tracker's performance by providing better signal excess at the tracker input through adaptive ping management. The formulation considers the aspects of the specular condition and Doppler information, by source and waveform selection and variable ping time interval. We also include sonar performance model, multistatic target tracker and ping contact simulator in our adaptive control architecture. The simulation examples illustrate the benefit of the adaptive ping schedule scheme and the viability of the approach. Future work will focus on comprehensive statistical Monte Carlo evaluation on a large multistatic field. We anticipate the need for intelligent grid-size selection and ping interval selection for more efficient computation.

References

[1] D. Grimmett, and S. Coraluppi, "Multistatic Active Sonar System Interoperability, Data Fusion, and Measures of Performance," *NURC Technical Report NURC-FR-2006-004*, Apr. 2006.

[2] D. W. Krout, M. A. El-Sharkawi, W. J. L. Fox, and M. U. Hazen, "Intelligent Ping Sequencing for Multistatic Sonar Systems," *Proc. of the 9th Intl. Conf. on Information Fusion*, Florence, Italy, Jul. 2006.

[3] A. Saksena, and I-J. Wang, "Dynamic Ping Optimization for Surveillance in Multistatic Sonar Buoy Networks with Energy Constraints," *Proc. of the 47th IEEE Conf. on Decision and Control*, Cancun, Mexico, Dec. 2008.

[4] D. Grimmett, "Multi-Sensor Placement to Exploit Complementary Properties of Diverse Sonar Waveforms," *Proc. of the 9th Intl. Conf. on Information Fusion*, Florence, Italy, Jul. 2006.

[5] D. Grimmett, S. Sullivan, Sr., and J. Alsup, "Modeling Specular Occurrence in Distributed Multistatic Fields," *Proc. of the IEEE Oceans'08 Conf.*, Kobe, Japan, Apr. 2008.

[6] D. Grimmett, "Multistatic Target Tracking using Specular Cue Initiation and Directed Data Retrieval," *Proc. of the 11th Intl. Conf. on Information Fusion*, Cologne, Germany, Jul. 2008.

[7] R. F. Gragg, "The BASIS-3D Acoustic Target Strength Model", *NRL/FR/7140–07-101052*, Washington D.C., U.S.A., Naval Research Laboratory, 2002.

[8] S. Coraluppi, and D. Grimmett, "Multistatic Sonar Tracking," *Proc. of the SPIE Conf. on Signal Processing, Sensor Fusion, and Target Recognition XII*, Orlando, Florida, Apr. 2003.

[9] S. Blackman, and R. Popoli, *Design and Analysis of Modern Tracking Systems*, Artech House, Norwood, MA, 1999.

[10] R. J. Urick, "Solving the Sonar Equations with Fluctuating Signals in Noise," *Proc. of IEEE Intl. Conf. on Acoustics Speech and Signal Processing*, May 1977.